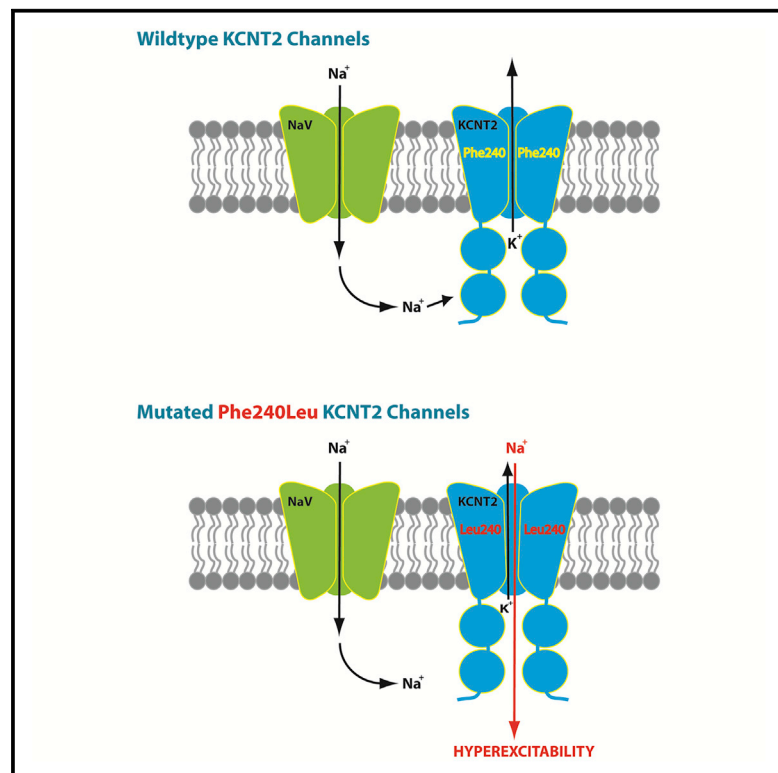# Cell Reports

A De Novo Mutation in the Sodium-Activated Potassium Channel KCNT2 Alters Ion Selectivity and Causes Epileptic Encephalopathy

Graphical Abstract

Authors

Sushmitha Gururaj,
Elizabeth Emma Palmer,
Garrett D. Sheehan, ..., Michael E. Duffey,
Ann Bye, Arin Bhattacharjee

Correspondence

ab68@buffalo.edu

In Brief

Gururaj et al. report a *KCNT2* mutation in a patient with epileptic encephalopathy and employ electrophysiological analyses to establish channel properties that could underlie epileptogenesis: namely, inhibition by high $[Cl^-]_i$ and loss of exclusive selectivity to K^+. Furthermore, primary neurons expressing Ph240Leu display a hyperexcitable phenotype.

Highlights

- We report a variant in the K_{Na} channel *KCNT2* linked to a human phenotype

- Phe240Leu channels are no longer predominantly permissive to only K^+

- Expressing Phe240Leu in primary neurons induces membrane hyperexcitability

- "Change-of-function" establishes pathogenicity of mutation in epileptic encephalopathy

CrossMark

CellPress

A De Novo Mutation in the Sodium-Activated Potassium Channel KCNT2 Alters Ion Selectivity and Causes Epileptic Encephalopathy

Sushmitha Gururaj,[1,9] Elizabeth Emma Palmer,[2,3,4,9] Garrett D. Sheehan,[1] Tejaswi Kandula,[2,3] Rebecca Macintosh,[2] Kevin Ying,[5] Paula Morris,[5] Jiang Tao,[5] Kerith-Rae Dias,[5] Ying Zhu,[4,6] Marcel E. Dinger,[3,5] Mark J. Cowley,[3,5] Edwin P. Kirk,[2,3,6] Tony Roscioli,[2,3,6] Rani Sachdev,[2,3] Michael E. Duffey,[7] Ann Bye,[2,3,10] and Arin Bhattacharjee[1,8,10,11,*]

[1]Pharmacology and Toxicology, University at Buffalo - The State University of New York, Buffalo, NY 14214, USA
[2]Sydney Children's Hospital, Randwick, NSW 2031, Australia
[3]University of New South Wales, Sydney, NSW 2031, Australia
[4]Genetics of Learning Disability Service, Waratah, NSW 2298, Australia
[5]Kinghorn Centre for Clinical Genomics, Garvan Institute of Medical Research, Sydney, NSW 2298, Australia
[6]SEALS Pathology, Randwick, NSW 2031, Australia
[7]Physiology and Biophysics, University at Buffalo - The State University of New York, Buffalo, NY 14214, USA
[8]Program for Neuroscience, University at Buffalo - The State University of New York, Buffalo, NY 14214, USA
[9]These authors contributed equally
[10]Senior author
[11]Lead Contact
*Correspondence: ab68@buffalo.edu
https://doi.org/10.1016/j.celrep.2017.09.088

SUMMARY

Early infantile epileptic encephalopathies (EOEE) are a debilitating spectrum of disorders associated with cognitive impairments. We present a clinical report of a *KCNT2* mutation in an EOEE patient. The de novo heterozygous variant Phe240Leu SLICK was identified by exome sequencing and confirmed by Sanger sequencing. Phe240Leu rSlick and hSLICK channels were electrophysiologically, heterologously characterized to reveal three significant alterations to channel function. First, $[Cl^-]_i$ sensitivity was reversed in Phe240Leu channels. Second, predominantly K^+-selective WT channels were made to favor Na^+ over K^+ by Phe240Leu. Third, and consequent to altered ion selectivity, Phe240Leu channels had larger inward conductance. Further, rSlick channels induced membrane hyperexcitability when expressed in primary neurons, resembling the cellular seizure phenotype. Taken together, our results confirm that Phe240Leu is a "change-of-function" *KCNT2* mutation, demonstrating unusual altered selectivity in K_{Na} channels. These findings establish pathogenicity of the Phe240Leu *KCNT2* mutation in the reported EOEE patient.

INTRODUCTION

Early infantile epileptic encephalopathy (EOEE) is characterized by intractable seizures and severe cognitive impairment and/or developmental delay (Berg et al., 2010). The incidence of EE is estimated to be 4.3 per 10,000 live births per year (Hino-Fukuyo et al., 2009), and the diagnosis is a devastating one, with a high burden of care for families and the health service, a significant risk of comorbidities and shortened lifespan (Khan and Al Baradie, 2012). Over 200 divergent genetic causes have been identified including pathogenic variants in ion channels, synaptic, regulatory, and developmental proteins (McTague et al., 2016; Tamsett et al., 2009). Despite next-generation sequencing approaches, which have the power to interrogate multiple genes, over 60% of children with EOEE remain without a genetic diagnosis (Helbig et al., 2016). Identifying additional genetic causes is therefore critically important, as a molecular diagnosis allows personalized management, such as guidance of choice of antiepileptic or metabolic treatment, appropriate health surveillance for recognized co-morbidities, accurate estimation of recurrence risk in the family, provision of "closure," and access to specific support groups for families (Berkovic, 2015).

KCNT1, encoding the K_{Na} channel SLACK ("sequence like calcium-activated K^+," Slo2.2), has recently emerged as a key genetic cause of EOEE, with gain-of-function variants increasing peak current amplitudes of SLACK channels 3- to 12-fold (Barcia et al., 2012; Heron et al., 2012; Martin et al., 2014). Variants of *KCNT2* (SLICK, "sequence like an intermediate conductance K^+," Slo2.1) have not been previously linked to a human phenotype despite ~74% gene sequence homology and postulated hetero-tetramerization between the two subunits in at least some brain regions (Lim et al., 2014; Chen et al., 2009; Bhattacharjee et al., 2003; Lim et al., 2016). Slick is set apart by its rapid activation kinetics, sensitivity to intracellular chloride and cell volume variations, slight sodium permeability, and selective localization in brain regions, such as the sub-plate of the cerebral cortex in utero and the hippocampus and cortex in the adult, suggesting that the channel plays an ongoing role in cerebral function (Oeschger et al., 2012; Bhattacharjee et al., 2002, 2003; Tejada et al., 2014; Rizzi et al., 2016).
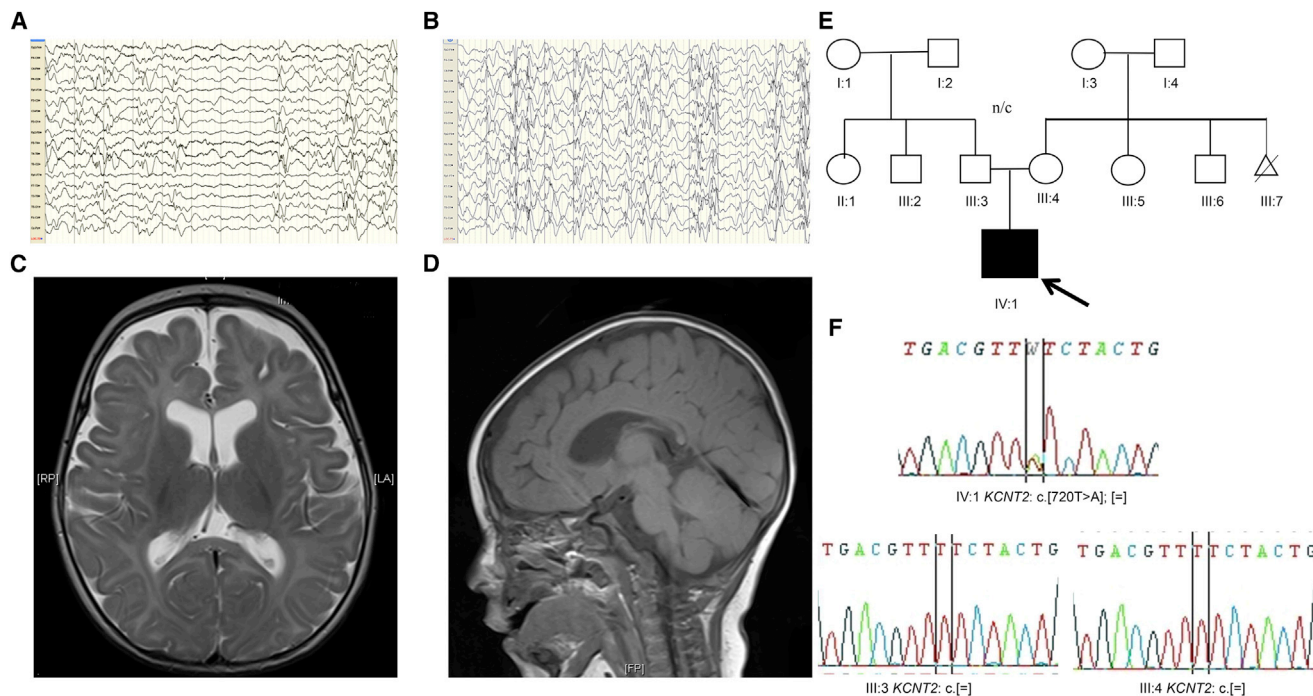
Figure 1. Clinical Presentation

(A and B) Representative electroencephalograms: longitudinal bipolar EEG montages (scale, 150 μV/cm) demonstrating high-voltage, posterior-dominant epileptiform activity, disorganized background, and decrements (5 months) (A) and high-voltage disorganized background and multifocal epileptiform activity consistent with hypsarrhythmia (1 year) (B).

(C and D) MRI brain images (5 months): Axial T2-weighted MRI demonstrating enlarged ventricles and extra-axial CSF spaces with thin corpus callosum (C). Sagittal T1 MRI showing thin corpus callosum (D).

(E and F) Pedigree (E) Sanger sequencing demonstrating de novo *KCNT2* variant (NM_001287819.1:c.[720T > A];p.[(Phe240Leu)];[=]) in proband (IV:1) (F).

EEG, electroencephalogram; MRI, magnetic resonance imaging. CSF, cerebrospinal fluid.

Brain MRI images were edited to remove all patient identifying information.

RESULTS AND DISCUSSION

We report a *KCNT2* variant in a male child with an EOEE phenotype consisting of neonatal hypotonia, profound developmental delay, and an intractable infantile-onset seizure disorder. The male proband is the only child of non-consanguineous parents with no pertinent family history. He was delivered at term following an uneventful pregnancy, although in retrospect his mother reported fetal hiccoughs. Growth parameters have been normal, and he has no dysmorphic features or congenital anomalies.

From 3 months of age, he had multiple daily episodes of staring with eye deviation to the left and single isolated jerks. At 4 months, he developed daily clusters of epileptic spasms lasting up to 8 min, and there was further regression in his development. His EE has been a lifelong feature (clinical and electrical). At the current age of 4 years, he has multiple daily seizures of mixed semiology that have remained resistant to polypharmacy as detailed in the Supplemental Information. The predominant symptom is a prolonged tonic seizure; he also has myoclonic jerks and atypical absences.

The electroencephalogram (EEG) has been persistently abnormal with a disorganized background, decrements, multifocal epileptogenic activity, or hypsarrhythmia (Figures 1A

and 1B). A brain MRI demonstrated a generalized reduction in white matter and thinning of the corpus callosum (Figures 1C and 1D).

Prior extensive neurometabolic and genetic investigations were non-diagnostic. Exome sequencing (ES) identified a non-synonymous variant in *KCNT2* (NM_001287819.1:c.[720T > A];p.[(Phe240Leu)];[=]) (Figure 1E), confirmed as de novo by bidirectional Sanger sequencing (Figure 1F). ES detected no other plausible variants in known EOEE genes. The affected residue is highly conserved, not listed in ExAC (last accessed July 2016) and in silico tools predicted pathogenicity (Supplemental Information). At the structural level, the residue Phe-240 is situated in the channel pore helix between transmembrane domains S5 and S6; it has been demonstrated by Garg et al. (2013) to be critical to normal Slick channel gating (Suzuki et al., 2016). Based on a SLO2.1 pore helix homology model, salient interactions between Phe-240 and the S5 and S6 domains of the Slick channel were predicted and subsequently electrophysiologically confirmed (Garg et al., 2013). Several Phe-240 variants showed constitutive activity as a function of substitute residue hydrophilicity, and, further, hydrophobic interactions between Phe-240 and S5 residues were essential to the stable-closed resting state of the channel (Suzuki et al., 2016). We therefore hypothesized that the Phe240Leu mutation alters channel function.
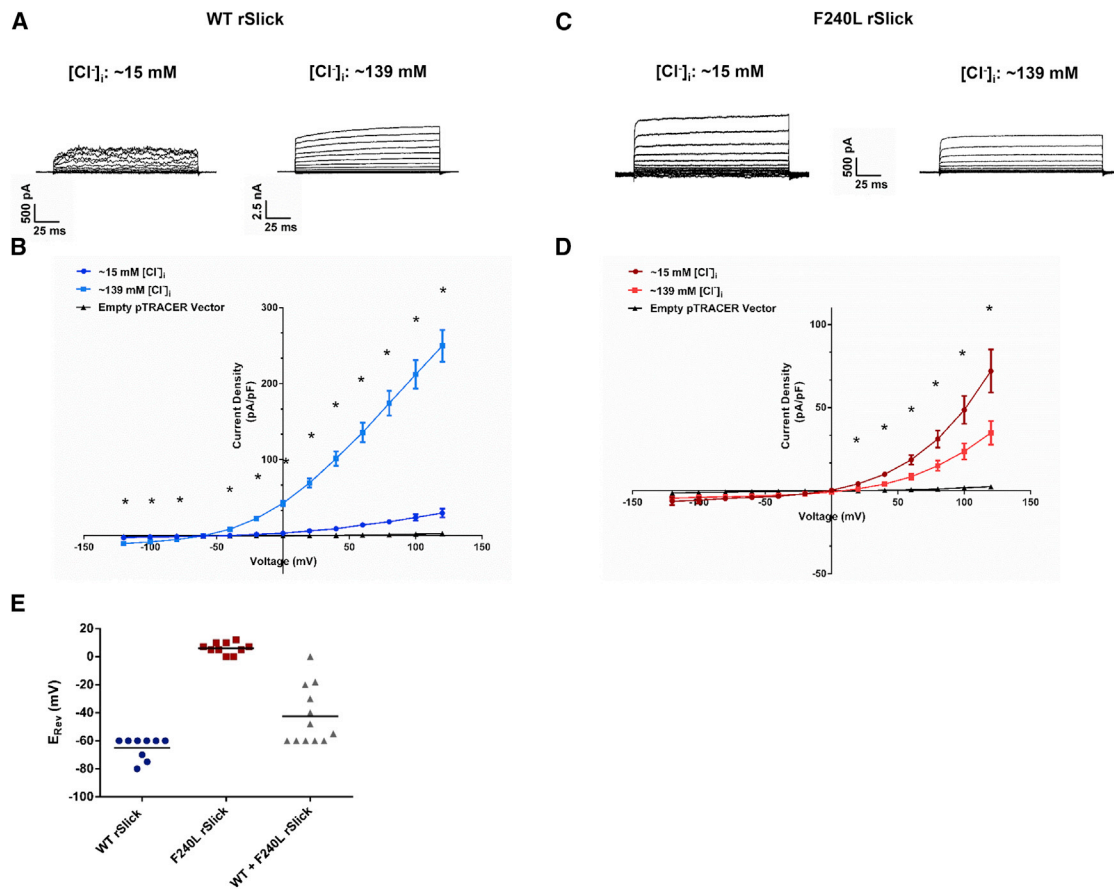
Figure 2. Phe240Leu Alters [Cl⁻]ᵢ Sensitivity and K⁺ Selectivity of rSlick Channels

(A and C) Representative whole-cell current traces evoked by depolarizing steps in pipette chloride concentration of ∼15 mM (left) or ∼139 mM (right) of WT rSlick (A) and F240L rSlick (C).

(B and D) Effect of increasing [Cl⁻]ᵢ concentration on current-voltage relationship of WT (B) and F240L I_{Slick} (D) (n = 7 per group). Unpaired t test, *p < 0.005. Error bars represent SEM.

(E) Scatterplot of reversal potentials (E$_{Rev}$) recorded in WT-, F240L-, and 1:1 WT+F240L-expressing CHO cells. Bars represent mean value per group (n = 12 per group). Data points reflect E$_{Rev}$ values across both ∼15 and ∼139 mM [Cl⁻]ᵢ.

To test the functional effect of the p.(Phe240Leu) variant, we recorded wild-type (WT) and Phe240Leu rSlick currents in Chinese hamster ovary (CHO) cells. Rat Slick channels in the pTRACER vector were used for this study following the failure of human SLICK pTRACER expression to produce detectable currents. The high sensitivity of rSlick channels to intracellular Cl⁻ was recapitulated by WT channels with a significant Cl⁻ dependent 4-fold increase in current density from ∼15 mM to ∼139 mM [Cl⁻]ᵢ in the presence of 13.2 mM [Na⁺]ᵢ (Figure 2A) (Bhattacharjee et al., 2003). Surprisingly, Phe240Leu channels showed a 3-fold decrease in current density from ∼15 to ∼139 mM [Cl⁻]ᵢ (Figure 2B). The model postulated by Garg et al. (2013) attributes constitutive activity of Phe-240 mutant channels to uncoupling of the C terminus from the channel pore helix. Although the region that confers Cl⁻ sensitivity is unknown, it could be speculated that the uncoupling of an intracellular site for Cl⁻ sensitivity from the activation gate would render the channel insensitive to Cl⁻ or uncover an inhibitory mechanism for Cl⁻. An alternative possibility is simply that WT and mutant channels undergo opposite regulation by Cl⁻.

Most strikingly, we observed a ∼60 mV shift in reversal potential (E$_{Rev}$) (0 mV) of Phe240Leu channels compared to WT (−60 mV) (Figure 2C), independent of [Cl⁻]ᵢ. This indicates that the predominantly K⁺-selective WT channel is converted into a channel of multi-ion nature by Phe240Leu, non-selective to K⁺ at the very least, and presumably permissive to Na⁺ (Joiner et al., 1998; Bhattacharjee et al., 2003). Of note, the −60 mV E$_{Rev}$ of WT Slick channels denotes the slight selectivity (1/20th of that of potassium) to sodium ions that Slick channels were originally characterized to possess, as an exclusively potassium-selective channel would have an E$_{Rev}$ much closer to predicted E$_K$ of ∼−73 mV (Bhattacharjee et al., 2003). When a 1:1 ratio of WT and Phe240Leu rSlick was expressed, a variable distribution of E$_{Rev}$ values was observed (Figure 2E). We speculate that this could imply assembly of variable stoichiometries of WT and Phe240Leu subunits into tetramers; the range of E$_{Rev}$ values corresponds to WT or Phe240Leu Slick homomers as well as
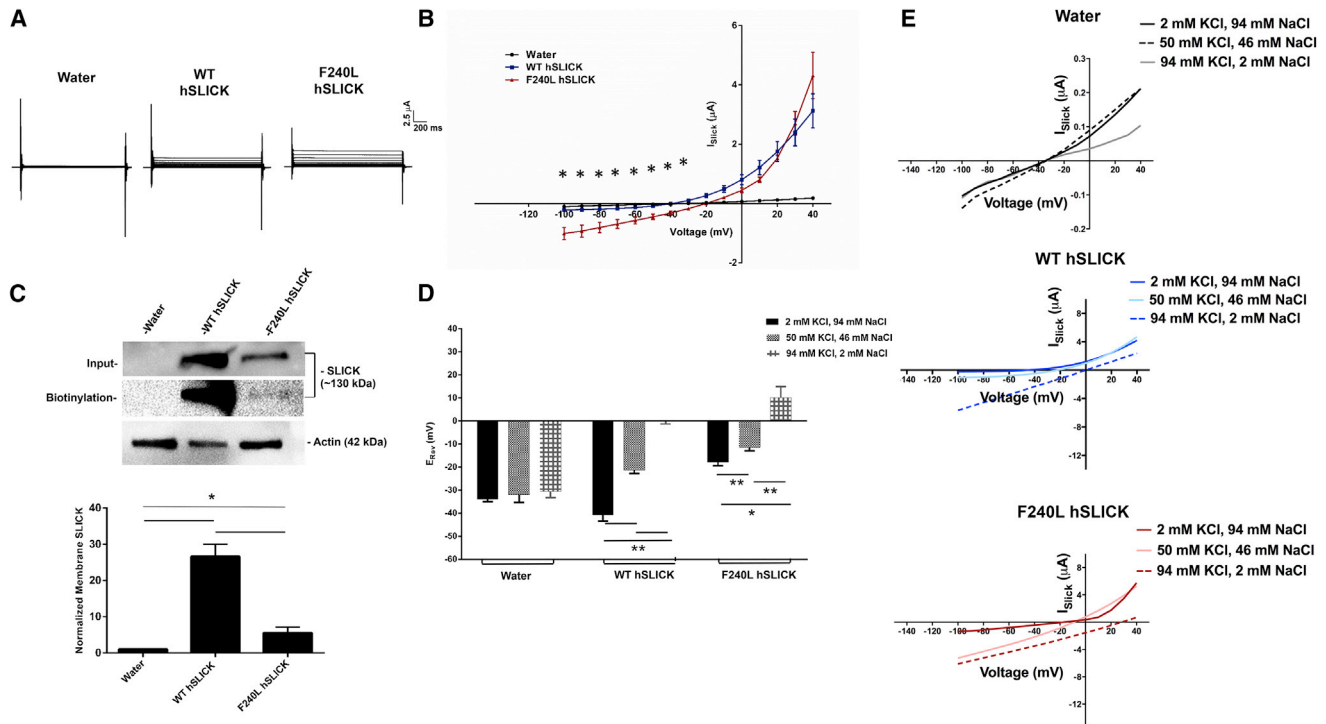
Figure 3. Phe240Leu Alters K⁺ Selectivity of hSLICK Channels
(A) Representative whole-cell oocyte current traces evoked by depolarizing steps.
(B) Effect of the F240L mutation on I_{Slick} current amplitudes recorded in injected oocytes (n = 5 per group per family). Unpaired t test, *p < 0.05. Error bars represent SEM.
(C) Top: representative western blot for membrane hSLICK in *Xenopus* oocytes. Actin was used as a loading control. Bottom: densitometric analysis of represented western blots for Slack quantified as normalized to actin. Data are expressed as mean ± SEM (n = 3 for all groups). Statistics performed using one-way ANOVA followed by multiple comparisons using Tukey's method (*p < 0.05). Error bars represent SEM.
(D) Relative reversal potentials (E_{Rev}) recorded in injected oocytes in ND-96 bath solution containing 2, 50, or 94 mM KCl during depolarizing voltage steps (n = 5 per group for water and WT hSLICK groups, n = 6 per group for Phe240leu hSLICK group). Error bars represent SEM.
(E) Representative I_{Slick} current amplitudes. Unpaired t test, **p < 0.005 between the 2 mM KCl and 50 mM KCl WT and F240L hSLICK groups, 2 mM KCl and 94 mM KCl WT F240L hSLICK groups, 50 mM KCl and 94 mM KCl WT and F240L hSLICK groups, *p < 0.05 between the 2mM KCl and 94 mM KCl F240L hSLICK groups. Shown are mean ± SEM. All recordings were performed in 500 μM NFA.
See also Figure S1.

WT: Phe240Leu heteromers, with the possible configurations being 1:3, 3:1, and 1:1. Nonetheless, since homomeric WT channels unvaryingly reverse at more negative potentials, heterozygous expression of Phe240Leu Slick, and presumably the Phe240Leu *KCNT2* allele, appears to be sufficient for altered channel properties and pathogenicity.

In *Xenopus laevis* oocytes, altered selectivity of Phe240Leu hSLICK channels was demonstrated by a ∼20 mV E_{Rev} shift toward E_{Na} (WT, −40 mV; Phe240Leu, −22 mV) and increased inward current (Figure 3B). Rat Phe240Leu Slick channels also displayed these altered properties in *Xenopus* oocytes (Figure S1). Membrane biotinylation assays showed high surface expression for WT hSLICK channels whereas Phe240Leu channels were only detected upon overexposure of signal (Figure 3C). In addition, Phe240Leu had low total protein levels, consistent with reduced membrane trafficking, translation of cRNA and/or rapid protein degradation. Phe240leu I_{Slick} being comparable to WT I_{Slick} despite poor expression suggests fewer but larger conducting mutant channels at the oocyte membrane. Whether

this is a result of mutation-induced alterations in pore helix structure facilitating increased conductance or open probability of single channels is unresolved from the present experiment design. Poorly expressed Phe-240 substitutions (Phe240Ser, Phe240Asn, and Phe240Cys) have been previously reported in *Xenopus* oocytes (Garg et al., 2013). Phe-240 is therefore critical not only to gating but also to normal membrane expression of hSLICK channels.

The exclusive selectivity of K_{Na} channels to K⁺ is vital to their physiological functions. Altered Phe240Leu ion selectivity was tested in *Xenopus* oocytes by partially replacing external Na⁺ with K⁺ over a range of concentrations (Figures 3D and 3E). WT channels demonstrated a significant depolarizing shift in E_{Rev}s from −40 mV (in 2 mM KCl) to −22 mV (in 50 mM KCl) to 0 mV (in 94 mM KCl) (mean of n = 5 for all groups), the latter most E_{Rev} in high K⁺ being evidence of a channel predominantly selective to potassium. In contrast, Phe240Leu channels reversed at positive voltages of 10 mV in 94 mM KCl bath solution (mean of n = 6 for all groups). Upon comparing empirically
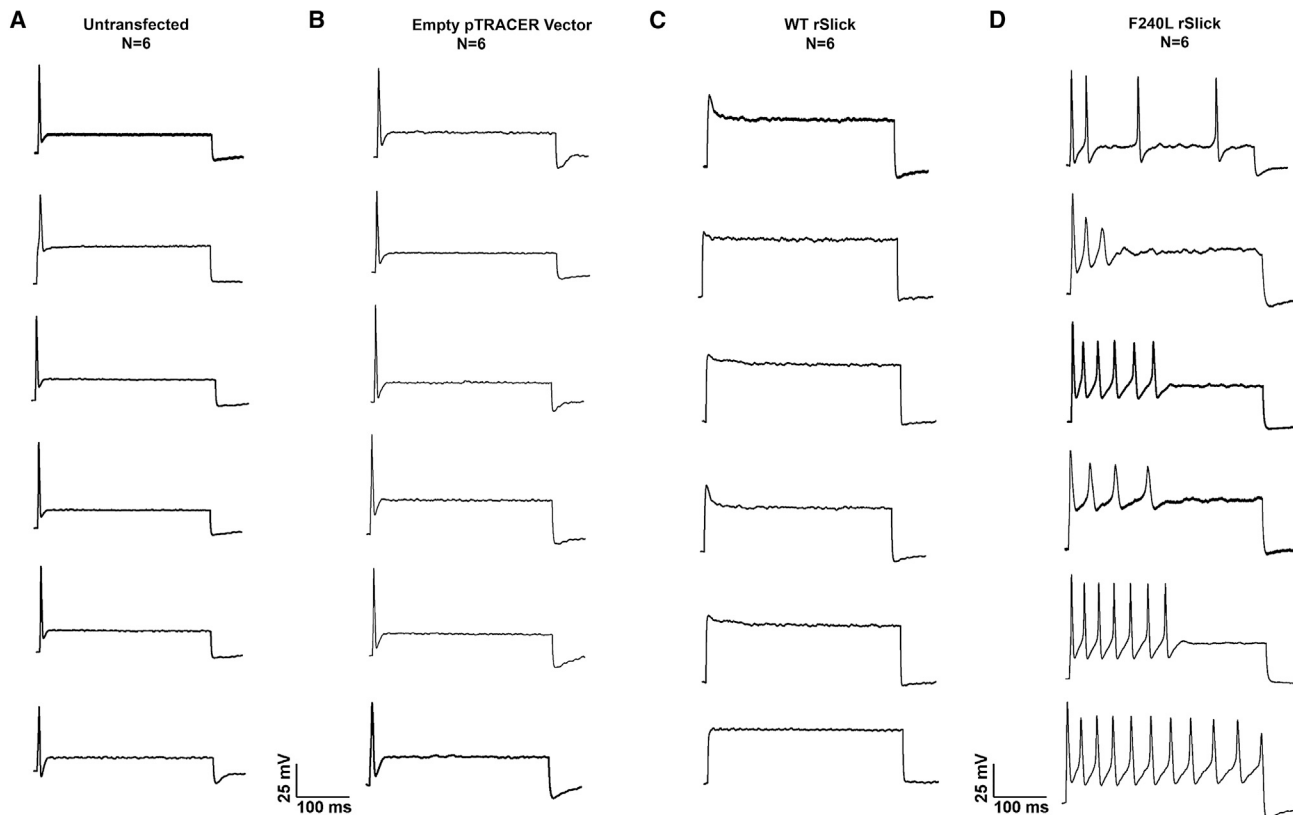
Figure 4. Overexpression of the *KCNT2* Phe240Leu Mutation Causes Membrane Hyperexcitability in Primary Neurons
(A–D) Representative action potential recordings of untransfected (A), empty pTRACER- (B), WT rSlick- (C), and F240L rSlick- (D) transfected neurons. Equal amounts (0.5 μg) of WT rSlick or Phe240Leu rSlick or empty pTRACER vector were transfected into embryonic rat DRG neurons plated on 18-mm glass coverslips. Whole-cell current clamp was performed 24–48 hr post-transfection. Current-clamp recordings were performed using an injection of a supra threshold stimulus of 400 pA for 1,000 ms. Shown are individual traces for a total n = 6 for the untransfected, pTRACER-, WT rSlick-, and F240L rSlick-transfected groups.

obtained E_{Rev} values with theoretical predictions of the Nernst Potential, we found that in high external K$^+$, the WT E_{Rev} of ∼0 mV is similar to the predicted value of ∼−3 mV whereas the F240L E_{Rev} of ∼+10 mV is significantly depolarized in comparison, indicative of an altered selectivity of mutant channels favoring sodium ions over potassium. Together, these findings indicate loss of predominant selectivity to K$^+$ in Phe240Leu channels and, likely, permeability to Na$^+$.

To demonstrate physiological causality of the Phe240Leu mutation toward the epilepsy phenotype, membrane properties of primary neurons overexpressing WT or F240L rSlick were examined. Primary embryonic rat dorsal root ganglion (DRG) neurons were chosen for this experiment because they possess homogeneous firing properties resembling adult primary neurons and express the complete subset of membrane proteins necessary for intrinsic membrane plasticity and action potential propagation (Tamsett et al., 2009; Grigaliunas et al., 2002). Our first observation was that F240L rSlick induced neuronal toxicity and resulted in exclusion of the majority of GFP-positive neurons from analysis, wherein exclusion criteria were cell death or inability to successfully seal or break in during patch clamp experiments. This is reflected in that fact that a total of 88 individual attempts (∼6.8%) to record GFP-positive cells were

made to obtain the reported n of 6 (Figure 4D). In comparison, empty pTRACER- and WT rSlick-transfected neurons showed lesser toxicity (n = 6 of 25 individual attempts [24%] to record cells), demonstrating pathogenicity of mutant channel overexpression (Figures 4B and 4C). Second, we found the mutation to induce distinct alterations in firing properties. WT rSlick-transfected neurons were unable to fire complete action potentials as would be predicted for the overexpression of a large conductance, rapidly activating K$^+$ channel (Bhattacharjee et al., 2003); indeed, the rapid activation kinetics of Slick were predicted to affect action potential formation using neuronal simulations (Bhattacharjee et al., 2005). F240L rSlick induced repetitive firing during current injection which was in clear contrast to untransfected and empty vector-transfected neurons that unequivocally fired a single action potential, as has previously been established as characteristic of the primary DRG neuronal model (Grigaliunas et al., 2002; Toman et al., 2004; Nuwer et al., 2010). These results indicate that the Phe240Leu mutation causes membrane hyperexcitability—a cellular hallmark of the epilepsy phenotype—in DRG neurons. Our in vitro observations in combination with the in vivo patient information demonstrate severe pathogenicity of heterozygous expression of the mutation, limiting further physiological testing

of the mutation in an in vivo animal model. Nonetheless, it is conceivable that the functional neuronal findings of increased membrane excitability contribute to the cellular manifestation of the epileptic phenotype.

This work characterizes Phe240Leu as a "change-in-function" de novo mutation. The variant alters a K^+-channel upregulated by Cl^- into a Na^+-channel downregulated by Cl^-. We present genetic and functional evidence that supports the pathogenicity of the p.(Phe240Leu) variant in the proband. Non-selectivity to K^+ has been previously reported with a mutation in the inward rectifying GIRK2 channel in the *weaver* mouse (Slesinger et al., 1996); however, the present study reports a *KCNT2* mutation in humans.

Despite high-sequence homology and structural similarities, KCNT1 and KCNT2 channels appear to have very different roles in physiological as well as pathophysiological conditions, likely resulting from distinct, often non-overlapping, patterns of localization within the central and peripheral nervous system (Bhattacharjee et al., 2002, 2003; Rizzi et al., 2016; Tomasello et al., 2015). Thus, it follows that while gain-of-function *KCNT1* epilepsy mutations reported thus far are proposed to selectively enhance K^+ currents, resulting in inhibitory neuronal suppression (Barcia et al., 2012; Kim and Kaczmarek, 2014), the Phe240Leu *KCNT2* mutation suggests a uniquely contrasting mechanism whereby increased inward I_{Na} may affect the precisely synchronized Na^+ and K^+ exchange that is crucial to normal intrinsic neuronal excitability. Interestingly a gain-of-function mutation in the voltage-gated sodium channel $Na_V1.2$-encoding *SCN2A* has been shown to cause hyper-excitability in utero (Scalmani et al., 2006), and *SCN2A* variants are an important genetic cause of EOEE.

In conclusion, we present empirical evidence for functional pathogenicity of a K_{Na} channel mutation associated with epilepsy in a physiologically relevant cellular model, namely, primary cultured neurons. It is therefore readily conceivable that increased SLICK (Phe240Leu)-dependent Na^+ currents in selective neuronal populations, such as in excitatory neurons of the hippocampus, contribute to epileptogenesis.

EXPERIMENTAL PROCEDURES

Subjects

The proband was enrolled, with his parents, in a trio exome sequencing project performed at the Garvan Institute as part of a cohort of 31 patients with EE and coordinated by SEALS molecular genetics laboratory and the Departments of Clinical Genetics and Paediatric Neurology at Sydney Children's Hospital as previously described (Palmer et al., 2015). Informed consent for exome sequencing was obtained from all participants or their guardians as approved by the ethics committee from The Sydney Children's Hospital Network and the Prince of Wales Hospital Campus, Sydney, Australia (Human Research Ethics Committee [HREC] ref. no. 13/094 and LNR/13/ SCHN/112).

Exome Sequencing and Sanger Confirmation

DNA was extracted from peripheral blood, and next-generation sequencing was performed using a Nextera rapid capture expanded exome kit, with libraries analyzed on an Illumina HiSeq2500. Reads were aligned to the Human Genome Reference Sequence Hg19/GRCh37 using Burrows-Wheeler Alignment (BWA)-MEM, and single nucleotide and short insertion/deletion variants were identified using HaplotypeCaller from GATK. Data filtering and variant prioritization were performed using the GEMINI platform as described previously (Palmer et al., 2015). Bidirectional Sanger sequencing was performed on DNA from the proband and both parents using standard methodology to verify and segregate candidate variants.

Cell Culture

CHO cells were cultured at 37°C in 5% CO_2 in an Iscove's Modified Dulbecco's Medium (IMDM) medium supplemented with 10% fetal bovine serum (FBS), 1% HT supplement (Life Technologies), and 1% penicillin-streptomycin. 1 day after plating at ~70% confluency, CHO cells were transiently transfected with 1 μg of either WT or mutated rSlick DNA in the expression plasmid pTRACER via lipofectamine (Invitrogen) and cultured for 48 hr. For the 1:1 WT: F240L Slick co-expression experiments, CHO cells were co-transfected with equal amounts (0.5 μg) of WT and mutated rSlick DNA. Cells were plated in 35-mm dishes for all electrophysiology and in 6-well plates for all biochemistry experiments.

Mutagenesis and RNA Preparation

Site-directed mutagenesis at Phe240 was performed using the QuikChange site-directed mutagenesis kit (Stratagene). The mutation Phe240Leu was engineered into rat Slick cDNA in pTRACER, rat Slick cDNA in pOX, and human Slick cDNA in psGEM using specific primer sets (Table S1). PfuTurbo-mediated PCR incorporation of the mutation(s) was followed by DpnI digestion to eliminate non-amplified cDNA. Remaining PCR products were transformed into XL-10 Gold Ultracompetent Cells (Agilent Technologies) and mini-prepped (QIAGEN Spin Mini-Prep Kit). The final products were sequence verified to confirm the sole mutation in the sequence to be Phe240Leu. Rat and human Slick cRNA was then prepared using the T3 and T7 mMessage kit, respectively (Ambion). Rat Kcnt2 cDNA in the pOX vector was kindly provided by J. Kronengold (Yale University), and human KCNT2 cDNA in the psGEM vector was kindly provided by M. Sanguinetti (University of Utah).

Preparation of Oocytes

Xenopus laevis oocytes from mature females were obtained and digested in OR3 solution containing collagenase. De-folliculated oocytes (stages 5–6) were injected with 75 ng rSlick (WT or Phe240Leu) cRNA or 150 ng hSLICK (WT or Phe240Leu) cRNA or water alone with the Nanoject Microinjection system (Drummond Scientific Co.). Oocytes were incubated at 18°C in OR3 medium for 2–3 days prior to functional analyses.

DRG Neuronal Culture

Female and adult timed pregnant Sprague Dawley rats (Harlan Laboratories) were used for all experiments. Animals were housed singly in a temperature and humidity-controlled animal facility on a 12 hr:12 hr light:dark schedule with food and water freely available. All procedures were approved by the University at Buffalo Institutional Animal Care and Use Committee and performed in accordance with NIH guidelines for the use of laboratory animals in research. On the day of the dissection, rats were euthanized by CO_2 asphyxiation and E15 embryos were extracted. DRG were dissected from the embryos and enzymatically digested with trypsin (2.5 mg/ml) at 37°C for 50 min, followed by mechanical dissociation and plating. DRG neurons were plated onto poly-D-lysine (Sigma; 100 mg/ml) and laminin- (Invitrogen; 3 mg/ml) coated coverslips. Cells were maintained at 37°C in a 7% CO_2-humidified incubator in serum-free medium, comprised of the trophic factors N2 (Gemini Bio products; 1%), L-glutamine (Invitrogen; 200 mg/ml), and nerve growth factor (NGF) (Harlan Laboratories; 100 ng/ml) in 50% DMEM and 50% F-12 (Nuwer et al., 2010). For 2 days after the day of the dissection, cells were cultured in C2 media containing the anti-mitotic cytosine β-D-arabinofuranoside hydrochloride (Sigma; 3 mM), followed by 2 days of recovery before use in experiments. Transient transfection of neurons with empty pTRACER vector, WT rSlick pTRACER, or F240L rSlick pTRACER was done on day 5 of culture using lipofectamine 2000 (Invitrogen). Recordings were taken 24–48 hr after transfection.

Electrophysiology
Two-Electrode Voltage-Clamp

Oocytes were voltage-clamped in a whole-cell mode configuration using a two-microelectrode oocyte clamp amplifier (OC-725A, Warner Instruments Corp.), and currents were digitized and recorded at room temperature. Microelectrodes with resistances of 0.5–2 MΩ (when filled with 1 M KCl) were fabricated from 1.5-mm outer diameter (O.D.) borosilicate glass tubing (TW150-4, World Precision Instruments) using a two-stage puller (Kopf Instruments) and

filled with 1 M KCl. The bath solution ND-96 contained (mM) 96 NaCl, 2 KCl, 1 $MgCl_2$, 1.8 $CaCl_2$, and 10 HEPES (pH 7.4). All recordings were performed in ND-96 containing 500 μM niflumic acid (NFA) to exclude endogenous $[Cl^-]_i$ conductance expressed in *Xenopus* oocytes. NFA is known to maximally activate Slick K_{Na} channels (EC_{50} ~2.1 mM), but, at much lower concentrations, it blocks Ca^{2+}-activated $[Cl^-]_i$ channels endogenously expressed by *Xenopus* oocytes (IC_{50} ~17 μM) (White and Aylwin, 1990; Dai et al., 2010). Oocytes were voltage clamped at a holding potential of −80 mV, and voltage steps from −100 mV to +40 mV were applied in 10 mV steps. Data were digitized and analyzed using pCLAMP 10.2 and analyzed using Clampex (Molecular Devices). Current-voltage relationships were determined by measuring currents at the end of the test pulses. Current traces were not leak or capacitance subtracted. Oocytes with resting membrane potentials more positive than −30 mV or with leaky currents were excluded.

Whole-Cell Patch Clamp

Glass electrodes were pulled using a horizontal pipette puller (Sutter Instrument Company) and fire polished to be of 5–12 MΩ resistance. Whole-cell voltage clamp recordings were performed on transfected CHO cells; whole-cell current clamp recordings were performed on transfected DRG neurons. Currents were recorded in voltage clamp mode at a holding potential of −70 mV, and voltage steps from −120 mV to +120 mV were applied in 20 mV steps. A current clamp protocol consisting of depolarizing steps in increments of 10 pA from −10 to 200 pA (20 ms duration) was used to record action potentials. Firing frequency was examined by measuring repetitive discharge of each cell upon injecting a supra threshold stimulus of 400 pA for 1,000 ms. Pipette offset was zeroed to account for tip potentials and capacitance compensation was used to limit series resistance errors.

The following solutions were used in these experiments.

For CHO cells:

Low-chloride pipette solution (in mM): 124 K-gluconate, 2 $MgCl_2$, 13.2 NaCl, 1 EGTA, 10 HEPES, 4 Mg-ATP, and 0.3 Na-GTP at pH 7.2.

High-chloride pipette solution (in mM): 124 KCl, 2 $MgCl_2$, 13.2 NaCl, 1 EGTA, 10 HEPES, 4 Mg-ATP, and 0.3 Na-GTP at pH 7.2.

Bath solution (in mM): 140 NaCl, 5.4 KCl, 1 $CaCl_2$, 1 $MgCl_2$, 10 HEPES, and 10 glucose.

For DRG neurons:

Pipette solution (in mM): 124 K-gluconate, 2 $MgCl_2$, 13.2 NaCl, 1 EGTA, 10 HEPES, 4 Mg-ATP, and 0.3 Na-GTP (pH 7.2).

Bath solution (in mM): 140 NaCl, 5.4 KCl, 1 $CaCl_2$, 1 $MgCl_2$, 15.6 HEPES, and 10 glucose (pH 7.4).

All data was acquired using the Axopatch 200B amplifier (Molecular Devices) and Multiclamp-700B (Molecular Devices), digitized, and filtered at 2 kHz. Data acquisition was monitored and controlled using pClamp 10.2 and analyzed using Clampex (Molecular Devices). Current-voltage relationships were determined by measuring currents at the end of the test pulses. Leaky currents were excluded from the analysis.

Membrane Biotinylation Assay

Cell-surface biotinylation on *Xenopus* oocytes was performed with the Pierce Cell Surface Protein Isolation Kit (Thermo Scientific) in accordance with the manufacturer's protocol. Briefly, 20 oocytes per group were washed with PBS and incubated with EZ-LINK Sulfo-NHS-SS-biotin for 30 min at 4°C followed by quenching solution. Oocytes were homogenized in lysis buffer (500 μl) containing protease inhibitor cocktail. An aliquot of the lysate was saved for western blotting for total protein. Biotinylated SLICK was isolated with NeutrAvidin agarose gel, eluted by sample buffer containing dithiothreitol. The resultant elute was loaded onto a Ready Gel, and western analysis was performed to detect membrane SLICK with monoclonal anti-Slick (UC Davis/NIH NeuroMab Clone NC 11/33). Signal was detected using horseradish peroxidase-conjugated mouse secondary antibody and chemiluminescent substrate kit (KPL). β-actin was used as a loading control.

Statistics

All electrophysiological analysis was performed using Clampfit 10 (Axon Instruments) and Origin (v.8.0) (Microcal Software). All statistical tests were performed using Prism (GraphPad). Data are shown as mean ± SEM. Confidence levels were calculated using Student's t test and ANOVA. The sample size for all experiments was least recordings required to detect significant differences and ensure reproducibility.

DATA AND SOFTWARE AVAILABILITY

The accession number for the Phe240Leu variant reported in this paper is ClinVar: 236299.

SUPPLEMENTAL INFORMATION

Supplemental Information includes Supplemental Information, one figure, and one table and can be found with this article online at https://doi.org/10.1016/j.celrep.2017.09.088.

AUTHOR CONTRIBUTIONS

S.G. performed all the experiments in the CHO cells, *Xenopus* oocytes, and primary neuronal cultures. E.E.P. performed the exome analysis, identified the *KCNT2* variant, and initiated collaboration with A. Bhattacharjee and team. G.D.S. helped perform electrophysiological recordings in CHO cells. T.R., A. Bye, R.S., E.P.K., E.E.P., and T.K. designed the exome study and recruited patients. T.R., M.E. Dinger, M.J.C., and Y.Z. designed the exome sequencing protocols and defined the bioinformatic analysis pathways. K.Y., P.M., J.T., and K.-R.D. performed the exome sequencing. T.R., R.S., and E.P.K. assisted in performing the genomic analyses. E.E.P. and T.K. collected phenotypic information. R.M. recruited patients. E.P.K. performed Sanger sequencing and supervised the assessment of the exome sequencing analysis. T.R. developed the genomic consent forms and ensured IRB accreditation for the study. M.E. Duffey helped perform all Xenopus oocyte experiments. A. Bhattacharjee designed the experiments in the CHO cells and *Xenopus* oocytes. The initial draft of the manuscript was written by A. Bhattacharjee, S.G., and E.E.P. and was edited by A. Bye, E.P.K., R.S., T.R., and M.E. Duffey All authors critically revised and gave final approval to this manuscript.

REFERENCES

Barcia, G., Fleming, M.R., Deligniere, A., Gazula, V.R., Brown, M.R., Langouet, M., Chen, H., Kronengold, J., Abhyankar, A., Cilio, R., et al. (2012). De novo gain-of-function KCNT1 channel mutations cause malignant migrating partial seizures of infancy. Nat. Genet. *44*, 1255–1259.

Berg, A.T., Berkovic, S.F., Brodie, M.J., Buchhalter, J., Cross, J.H., van Emde Boas, W., Engel, J., French, J., Glauser, T.A., Mathern, G.W., et al. (2010). Revised terminology and concepts for organization of seizures and epilepsies: report of the ILAE Commission on Classification and Terminology, 2005-2009. Epilepsia *51*, 676–685.

Berkovic, S.F. (2015). Genetics of epilepsy in clinical practice. Epilepsy Curr. *15*, 192–196.

Bhattacharjee, A., Gan, L., and Kaczmarek, L.K. (2002). Localization of the Slack potassium channel in the rat central nervous system. J. Comp. Neurol. *454*, 241–254.

Bhattacharjee, A., Joiner, W.J., Wu, M., Yang, Y., Sigworth, F.J., and Kaczmarek, L.K. (2003). Slick (Slo2.1), a rapidly-gating sodium-activated potassium channel inhibited by ATP. J. Neurosci. *23*, 11681–11691.

Bhattacharjee, A., von Hehn, C.A., Mei, X., and Kaczmarek, L.K. (2005). Localization of the Na+-activated K+ channel Slick in the rat central nervous system. J. Comp. Neurol. *484*, 80–92.

Chen, H., Kronengold, J., Yan, Y., Gazula, V.R., Brown, M.R., Ma, L., Ferreira, G., Yang, Y., Bhattacharjee, A., Sigworth, F.J., et al. (2009). The N-terminal domain of Slack determines the formation and trafficking of Slick/Slack heteromeric sodium-activated potassium channels. J. Neurosci. *29*, 5654–5665.

Dai, L., Garg, V., and Sanguinetti, M.C. (2010). Activation of Slo2.1 channels by niflumic acid. J. Gen. Physiol. *135*, 275–295.

Garg, P., Gardner, A., Garg, V., and Sanguinetti, M.C. (2013). Structural basis of ion permeation gating in Slo2.1 K+ channels. J. Gen. Physiol. *142*, 523–542.

Grigaliunas, A., Bradley, R.M., MacCallum, D.K., and Mistretta, C.M. (2002). Distinctive neurophysiological properties of embryonic trigeminal and geniculate neurons in culture. J. Neurophysiol. *88*, 2058–2074.

Helbig, K.L., Farwell Hagman, K.D., Shinde, D.N., Mroske, C., Powis, Z., Li, S., Tang, S., and Helbig, I. (2016). Diagnostic exome sequencing provides a molecular diagnosis for a significant proportion of patients with epilepsy. Genet. Med. *18*, 898–905.

Heron, S.E., Smith, K.R., Bahlo, M., Nobili, L., Kahana, E., Licchetta, L., Oliver, K.L., Mazarib, A., Afawi, Z., Korczyn, A., et al. (2012). Missense mutations in the sodium-gated potassium channel gene KCNT1 cause severe autosomal dominant nocturnal frontal lobe epilepsy. Nat. Genet. *44*, 1188–1190.

Hino-Fukuyo, N., Haginoya, K., Iinuma, K., Uematsu, M., and Tsuchiya, S. (2009). Neuroepidemiology of West syndrome and early infantile epileptic encephalopathy in Miyagi Prefecture, Japan. Epilepsy Res. *87*, 299–301.

Joiner, W.J., Tang, M.D., Wang, L.Y., Dworetzky, S.I., Boissard, C.G., Gan, L., Gribkoff, V.K., and Kaczmarek, L.K. (1998). Formation of intermediate-conductance calcium-activated potassium channels by interaction of Slack and Slo subunits. Nat. Neurosci. *1*, 462–469.

Khan, S., and Al Baradie, R. (2012). Epileptic encephalopathies: an overview. Epilepsy Res. Treat. *2012*, 403592.

Kim, G.E., and Kaczmarek, L.K. (2014). Emerging role of the KCNT1 Slack channel in intellectual disability. Front. Cell. Neurosci. *8*, 209.

Lim, E.T., Würtz, P., Havulinna, A.S., Palta, P., Tukiainen, T., Rehnström, K., Esko, T., Mägi, R., Inouye, M., Lappalainen, T., et al.; Sequencing Initiative Suomi (SISu) Project (2014). Distribution and medical impact of loss-of-function variants in the Finnish founder population. PLoS Genet. *10*, e1004494.

Lim, C.X., Ricos, M.G., Dibbens, L.M., and Heron, S.E. (2016). KCNT1 mutations in seizure disorders: the phenotypic spectrum and functional effects. J. Med. Genet. *53*, 217–225.

Martin, H.C., Kim, G.E., Pagnamenta, A.T., Murakami, Y., Carvill, G.L., Meyer, E., Copley, R.R., Rimmer, A., Barcia, G., Fleming, M.R., et al.; WGS500 Consortium (2014). Clinical whole-genome sequencing in severe early-onset epilepsy reveals new genes and improves molecular diagnosis. Hum. Mol. Genet. *23*, 3200–3211.

McTague, A., Howell, K.B., Cross, J.H., Kurian, M.A., and Scheffer, I.E. (2016). The genetic landscape of the epileptic encephalopathies of infancy and childhood. Lancet Neurol. *15*, 304–316.

Nuwer, M.O., Picchione, K.E., and Bhattacharjee, A. (2010). PKA-induced internalization of slack KNa channels produces dorsal root ganglion neuron hyperexcitability. J. Neurosci. *30*, 14165–14172.

Oeschger, F.M., Wang, W.Z., Lee, S., García-Moreno, F., Goffinet, A.M., Arbonés, M.L., Rakic, S., and Molnár, Z. (2012). Gene expression analysis of the embryonic subplate. Cereb. Cortex *22*, 1343–1359.

Palmer, E.E., Hayner, J., Sachdev, R., Cardamone, M., Kandula, T., Morris, P., Dias, K.R., Tao, J., Miller, D., Zhu, Y., et al. (2015). Asparagine synthetase deficiency causes reduced proliferation of cells under conditions of limited asparagine. Mol. Genet. Metab. *116*, 178–186.

Rizzi, S., Knaus, H.G., and Schwarzer, C. (2016). Differential distribution of the sodium-activated potassium channels slick and slack in mouse brain. J. Comp. Neurol. *524*, 2093–2116.

Scalmani, P., Rusconi, R., Armatura, E., Zara, F., Avanzini, G., Franceschetti, S., and Mantegazza, M. (2006). Effects in neocortical neurons of mutations of the Na(v)1.2 Na+ channel causing benign familial neonatal-infantile seizures. J. Neurosci. *26*, 10100–10109.

Slesinger, P.A., Patil, N., Liao, Y.J., Jan, Y.N., Jan, L.Y., and Cox, D.R. (1996). Functional effects of the mouse weaver mutation on G protein-gated inwardly rectifying K+ channels. Neuron *16*, 321–331.

Suzuki, T., Hansen, A., and Sanguinetti, M.C. (2016). Hydrophobic interactions between the S5 segment and the pore helix stabilizes the closed state of Slo2.1 potassium channels. Biochim. Biophys. Acta *1858*, 783–792.

Tamsett, T.J., Picchione, K.E., and Bhattacharjee, A. (2009). NAD+ activates KNa channels in dorsal root ganglion neurons. J. Neurosci. *29*, 5127–5134.

Tejada, M.A., Stople, K., Hammami Bomholtz, S., Meinild, A.K., Poulsen, A.N., and Klaerke, D.A. (2014). Cell volume changes regulate slick (Slo2.1), but not slack (Slo2.2) K+ channels. PLoS ONE *9*, e110833.

Toman, R.E., Payne, S.G., Watterson, K.R., Maceyka, M., Lee, N.H., Milstien, S., Bigbee, J.W., and Spiegel, S. (2004). Differential transactivation of sphingosine-1-phosphate receptors modulates NGF-induced neurite extension. J. Cell Biol. *166*, 381–392.

Tomasello, D.L., Gancarz-Kausch, A.M., Dietz, D.M., and Bhattacharjee, A. (2015). Transcriptional regulation of the sodium-activated potassium channel SLICK (KCNT2) promoter by nuclear factor-κB. J. Biol. Chem. *290*, 18575–18583.

White, M.M., and Aylwin, M. (1990). Niflumic and flufenamic acids are potent reversible blockers of Ca2(+)-activated Cl- channels in Xenopus oocytes. Mol. Pharmacol. *37*, 720–724.